

# Geochemical and Nd, Pb, and Sr Isotope Data from Deccan Alkaline Complexes—Inferences for Mantle Sources and Plume–Lithosphere Interaction

A. SIMONETTI<sup>1,\*</sup>, S. L. GOLDSTEIN<sup>1,†</sup>, S. S. SCHMIDBERGER<sup>2</sup>  
AND S. G. VILADKAR<sup>3</sup>

<sup>1</sup>MAX-PLANCK-INSTITUT FÜR CHEMIE, ABTEILUNG GEOCHEMIE, POSTFACH 3060, 55020 MAINZ, GERMANY

<sup>2</sup>DEPARTMENT OF EARTH AND PLANETARY SCIENCES, MCGILL UNIVERSITY, 3450 UNIVERSITY STREET, MONTRÉAL, QUÉBEC, CANADA, H3A 2A7

<sup>3</sup>DEPARTMENT OF GEOLOGY, ST XAVIER'S COLLEGE, BOMBAY 400 001, INDIA

RECEIVED OCTOBER 1, 1997; REVISED TYPESCRIPT ACCEPTED MAY 21, 1998

*Previous chemical and isotopic studies based on alkaline rocks and carbonatites associated with large, continental flood basaltic provinces indicate their important role in monitoring plume–lithosphere interaction. We report new major and trace element data, and Nd, Pb, and Sr isotope ratios for various alkaline silica-undersaturated rocks and carbonatites from several Deccan alkaline complexes in an attempt to evaluate the relative contributions of Réunion plume and Indian sub-continental mantles in their source regions. Major and trace element abundances for the most primitive silicate samples are consistent with an origin via small-degree partial melting of metasomatized mantle. Initial  $^{87}\text{Sr}/^{86}\text{Sr}$ ,  $^{143}\text{Nd}/^{144}\text{Nd}$  and Pb isotope ratios for the most primitive alkaline silicate samples and associated carbonatites exhibit a large variation, and are attributed to mixing of three distinct mantle components—Réunion plume, continental lithosphere and asthenosphere (Indian MORB-like). For the silicate rocks, isotope ratios correlate with major and trace element composition and support derivation from distinct mantle sources. The data obtained here are consistent with previous models invoking Réunion plume–continental lithosphere interaction to explain the origin of Deccan alkaline complexes, which suggest a more prominent role of Réunion mantle during the early stages of Deccan volcanism involving small-degree melting of plume-modified lithosphere. With time, the isotope systematics of both alkaline and tholeiitic magmatism record a larger lithospheric imprint.*

KEY WORDS: carbonatite; Deccan province; lithosphere; mantle plume; Réunion

## INTRODUCTION

Although the exact origin of carbonatite magma has yet to be agreed upon, whether derived via liquid immiscibility (e.g. Kjarsgaard & Hamilton, 1989; Church & Jones, 1995; Jones *et al.*, 1995; Kjarsgaard *et al.*, 1995), magmatic separation from a carbonated parental silicate magma or primary carbonatite melt (e.g. Wallace & Green, 1988; Dalton & Wood, 1993), the similarity between the Nd, Pb, and Sr isotope data from young (<200 Ma) carbonatites world wide and ocean island basalts (OIBs) clearly points to their mantle origin (e.g. Bell & Blenkinsop, 1987a, 1987b; Nelson *et al.*, 1988; Tilton & Bell, 1994). Recent Nd, Pb, and Sr isotope data from East African complexes, however, have led to questioning of the validity of some of these models, as these data indicate that (1) carbonatites and associated silicate rocks evolve along separate melt differentiation pathways, and (2) both represent discrete, partial melts derived from an isotopically heterogeneous mantle source consisting of HIMU and EMI components (e.g. Napak,

\*Corresponding author. Present address: Centre de recherche GEOTOP, Université du Québec à Montréal, succursale Centre-ville, CP 8888, Montréal, Québec, Canada, H3C 3P8. Telephone: (514) 987-3000, ext. 7019. Fax: (514) 987-3635. e-mail: c3204@er.uqam.ca

†Present address: Lamont–Doherty Earth Observatory of Columbia University, Palisades, NY 10964, USA.

Simonetti & Bell, 1994a; Mount Elgon, Simonetti & Bell, 1995; Oldoinyo Lengai, Bell & Dawson, 1995). In addition, Bell & Simonetti (1996) proposed that the variations in Nd, Pb, and Sr isotope ratios from East African carbonatites may be attributed to interaction between old, radiogenic continental lithosphere (EMI-like mantle component) and upwelling ('plume'), HIMU-like mantle.

Other studies have also proposed the involvement (both direct and indirect) of mantle plumes in carbonatite genesis (e.g. for the Cape Verdes, Gerlach *et al.*, 1988; the Canary Islands, Hoernle & Tilton, 1991; Brazil, Toyoda *et al.*, 1994; Huang *et al.*, 1995; Namibia, le Roex & Lanyon, 1998). The link between mantle plume activity and alkaline-carbonatite magmatism is further supported by the spatial relationship of carbonatite occurrences within flood basaltic provinces. Examples include those found in Brazil and Namibia associated with Paraná-Etendeka volcanism, those in Canada associated with Keeweenawan volcanism, and those in India associated with Deccan volcanism. In the Nd, Pb, and Sr isotope study of the Amba Dongar carbonatite complex from west-central India, Simonetti *et al.* (1995) proposed that the Réunion 'hotspot', responsible for the generation of the voluminous Deccan Traps, may have been involved in producing the parental melt to the Amba Dongar carbonatite.

The Deccan igneous province consists of a volumetrically large succession of predominantly tholeiitic lava flows ( $\sim 0.5 \times 10^6 \text{ km}^2$ ), which mark the first surface expression of the Réunion hotspot on the Indian subcontinent (Vandamme *et al.*, 1991). Geochronological data define the main period of Deccan flood basaltic volcanism at  $\sim 66 \text{ Ma}$  (e.g. Courtillot *et al.*, 1988; Duncan & Pyle, 1988; Vandamme *et al.*, 1991; Venkatesan *et al.*, 1993; Baksi, 1994) and suggest that volcanic activity occurred over a time interval of probably  $< 1 \text{ my}$  (Courtillot *et al.*, 1986a, 1986b). Devey & Stephens (1992) proposed that Deccan alkaline magmatism post-dated tholeiitic volcanism by up to 3 my. More recent  $^{40}\text{Ar}/^{39}\text{Ar}$  ages for several of the Deccan alkaline complexes examined in this study are listed in Table 1, and their locations are shown in Fig. 1. These ages clearly show that Deccan alkaline magmatic activity overlapped with the main period of tholeiitic volcanism. Moreover, on the basis of  $^{40}\text{Ar}/^{39}\text{Ar}$  ages, Basu *et al.* (1993) concluded that Deccan alkaline magmatism was slightly older ( $\sim 3 \text{ my}$  older) in the northern part of the province ( $\sim 68.5 \text{ Ma}$  for Barmer and Mundwara) compared with areas further south (e.g.  $\sim 65 \text{ Ma}$  for Phenai Mata). Figure 1 also shows that occurrences of alkaline magmatism are mainly restricted to the northern part of the Deccan igneous province, north of the Narmada Rift Valley. A summary of the geological settings and petrography of

the samples investigated in this study is provided in Table 1.

We report new geochemical and Nd, Pb, and Sr isotope data for various silica-undersaturated rocks and carbonatites from the Deccan alkaline complexes of Barmer, Bhuj, Mundwara and Amba Dongar. The main objectives are (1) to characterize the chemical and isotopic nature of the mantle responsible for derivation of the Deccan alkaline complexes, and (2) to evaluate the role of Réunion 'plume'-type mantle-lithosphere interaction, and to assess their respective contributions in the generation of Deccan alkaline magmatism.

## ANALYTICAL METHODS

Samples selected for chemical and isotopic analyses contained little or no evidence of subsolidus alteration. Before acid digestion, all sample powders (between 0.1 and 0.2 g) were spiked with two mixed isotope tracer solutions, one for  $^{87}\text{Rb}$ - $^{84}\text{Sr}$  and the other for  $^{150}\text{Nd}$ - $^{149}\text{Sm}$ . For silicate rocks, the sample powder was treated with a mixture of concentrated HF-HNO<sub>3</sub> in a Savillex vial and left at 140°C for a period of at least 48 h. Acid digestion of carbonatite samples involved a mixture of 6 N HCl and concentrated HNO<sub>3</sub> placed in a Savillex vial, also for 48 h. Procedures for chemical separation of Sr and Nd were similar to those described by White & Patchett (1984). Sr aliquots were loaded using a TaF solution on single W filaments, whereas Nd was loaded with HCl using a double Re filament technique. Nd and Sr isotope measurements were obtained by thermal ionization mass spectrometry at the Max-Planck-Institut für Chemie (Mainz) using a MAT 261 mass spectrometer operated in the static multicollection mode. Separation of lead was done using anion-exchange chromatography (after Manhès *et al.*, 1980), and U and Th determination followed the technique of Edwards *et al.* (1986), both conducted at GEOTOP, Université du Québec à Montréal. Lead, thorium and uranium concentrations were determined by isotope dilution using  $^{206}\text{Pb}$ ,  $^{229}\text{Th}$ , and  $^{233}\text{U}$ - $^{236}\text{U}$  spikes. Pb isotope measurements were obtained using either a single Faraday cage detector or Daly analogue detector (in peak switching mode), whereas U and Th were measured using an ion-counting Daly detector.

## RESULTS

### Mineral analyses

Representative average microprobe analyses of olivine and clinopyroxene phenocrysts from a basanite from Bhuj (95-BHJ-016) and a melilitite from Barmer (95-BMR-037) are listed in Tables 2 and 3. In addition,

Table 1: Summary of geology and petrography of Deccan alkaline complexes

Locality	Age (Ma)	Rock types and setting	Petrography	Country rocks	Reference
Bhuj	64.4–67.7 (1)	Plugs or sheet-like bodies of basanite–alkaline basalt (~100s of metres to 0.5 km in diameter), which cover an area of ~1000 km <sup>2</sup>	Lavas are characterized by a fine- to medium-grained porphyritic texture with phenocrysts (10–20 modal %) of olivine, Fe oxides, and strongly zoned clinopyroxene set in a fine-grained matrix consisting of olivine, clinopyroxene, biotite, microlites of nepheline and opaque oxides	Jurassic sandstone	4
Barmer (Sarnu- Dandali)	68.57 ± 0.08 (2)	Outcrops are small, scattered plug-like bodies of alkali pyroxenite, mela-nephelinite, ijolite and melilitite, which cover an area of ~200 km <sup>2</sup> ; these are typically intruded by thin dykes (~1 m) of REE-enriched carbonatite, syenite and phonolite	Nephelinite and melilitite are characterized by a microporphyritic texture with strongly zoned phenocrysts of diopside and olivine set in a fine-grained groundmass consisting predominantly of diopside, magnetite and nepheline. Phonolites are either strongly porphyritic containing phenocrysts of clinopyroxene, nepheline and sanidine ± titaniferous magnetite, or leucocratic, aphyric (glassy) with trachytic texture defined by feldspar laths ± clinopyroxene and nepheline	Rhyolitic lava and tuff of the Malani series (~745 Ma) and/or lower Cretaceous sediments (~120 Ma)	5, 6
Mundwara	68.53 ± 0.16 (2)	Igneous complex consists of three individual plutons (Musala, Mer and Toa Hills) occupying an area of ~12 km <sup>2</sup> . Each consists of a complete suite of alkaline mafic to felsic derivatives exhibiting complex intrusive relationships. Carbonatite dykes occur at the periphery of the plutons and represent a small volumetric amount (<1%) of the complex	Nephelinite, phonolite and tephrite are mainly characterized by a fine- to medium-grained, porphyritic texture containing predominantly phenocrysts (in varying proportions) of olivine, highly zoned diopside, Fe oxides, biotite, feldspar ± microphenocrysts of apatite and titanite (e.g. 95-MUN-030) set in an aphyric groundmass. Plutonic rocks (e.g. 95-MUN-028, –029) are medium to coarse grained, containing amphibole, biotite, feldspar, nepheline, Fe-oxides, clinopyroxene and ubiquitous apatite	Late Proterozoic granitic basement associated with the Cambay rift zone	7, 8
Amba Dongar	61 ± 2 (3) 76 ± 2 (3)	The carbonatite crops out as a ring-dyke structure consisting of an innermost ring of carbonatite breccia rimmed by calciocarbonatite, and these are intruded by ferrocarbonatite plugs and dykes. Associated alkaline silicate rocks consist of a central basanite plug (post-carbonatite), and plugs of nephelinite and phonolite	95-AMDO-001 is a fine-grained basanite containing clinopyroxene, nepheline, plagioclase and olivine, retrieved from the central plug of the complex; 95-AMDO-002 is an enclave of calciocarbonatite from a dyke of ferrocarbonatite breccia located 5 km northwest of Amba Dongar	Cretaceous sandstone and limestone of the Bagh formation, Deccan basalt and Precambrian Dharwar basement	9, 10

References: 1, Pande *et al.* (1988); 2, Basu *et al.* (1993); 3, Deans *et al.* (1972); 4, Krishnamurthy *et al.* (1988); 5, Chandrasekaran *et al.* (1990); 6, Wall *et al.* (1993); 7, Le Bas & Srivastava (1989); 8, Subrahmanyam & Leelanandam (1991); 9, Viladkar (1981); 10, Gwalani *et al.* (1993).

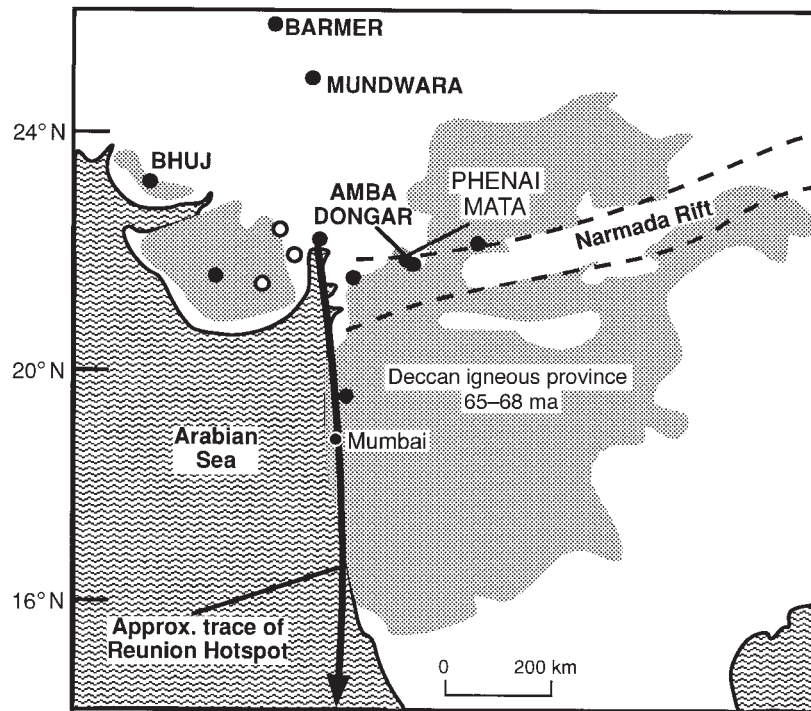


**Fig. 1.** Map of northwest-central India showing extent of Deccan igneous province (shaded area), the Narmada Rift Valley (dashed lines), and locations of associated alkaline complexes (●) examined in this study; these include Amba Dongar, Barmer, Bhuj, and Mundwara. Also shown are sample locations (○) for mildly alkaline picrites and basaltic flows (from Peng & Mahoney, 1995). The arrow marks the approximate path of Réunion plume in the Late Cretaceous (Campbell & Griffiths, 1990).

representative average compositions for clinopyroxene phenocrysts from an ijolite from Mundwara (95-MUN-028) are shown in Table 3. The olivines in the samples from Bhuj and Barmer are characterized by high Fo contents (81–90), with those for the latter being slightly less Fo rich. The compositions of the clinopyroxene phenocrysts (Table 3) correspond to those for diopside, and the range in *mg*-numbers (89–92) is restricted for samples from Bhuj and Barmer; in comparison, those from Mundwara suggest crystallization from a slightly more differentiated melt (*mg*-numbers 84–86).

### Chemical data

Table 4 lists X-ray fluorescence (XRF) whole-rock chemical analyses of samples examined in this study. With the exception of the phonolites, the remaining silicate samples contain moderately high MgO contents >6 wt %, corresponding to *mg*-numbers  $\{100[\text{atomic Mg}/(\text{Mg} + \text{Fe}^{2+})]\}$  ranging from 54 to 71, indicative of their relatively primitive nature. Figure 2 shows the variations in the contents of several major element oxides vs *mg*-number. Also shown in Fig. 2 for comparison are data for olivine basalts (primitive shield phase) and for the

differentiated series (gabbro, basalt, syenite) from the Piton des Neiges volcano, Réunion (Fisk *et al.*, 1988). With the exception of the data for the melilitites from Barmer and for the more differentiated samples (*mg*-number <40) from the Deccan alkaline complexes, those for the remaining samples overlap the trends defined by the samples from Réunion (Fig. 2). Of interest in Fig. 2, the melilitites from Barmer contain significantly higher  $\text{CaO}/\text{Al}_2\text{O}_3$  (>1.29) ratios and  $\text{TiO}_2$  contents (>5.8 wt %) compared with the remaining Deccan alkaline samples at similar *mg*-numbers.

The samples of basanite–nephelinite from Bhuj contain the highest abundances of both Ni (168–332 ppm) and Cr (429–995 ppm), and these are negatively correlated with *mg*-numbers (Fig. 3). Similar arrays are also defined by the data from Réunion (Fig. 3). For samples from Barmer and Bhuj with *mg*-number >50, the arrays shown in Fig. 3 are consistent with melt differentiation involving predominantly clinopyroxene and olivine fractional crystallization, a feature confirmed by both their phenocryst assemblage (Tables 1–3) and by results from melt experiments using lavas from Réunion (Fisk *et al.*, 1988). Variations in the abundances of incompatible trace elements, such as Zr and Rb, with melt differentiation

Table 2: Representative average microprobe analyses of olivine phenocrysts for samples from Bhuj and Barmer

Sample:	95-BHUJ-016								95-BMR-037			
Grain no.:	1	2	3	4	5	6	7	8	1	2	3	4
No. of analyses:	2	3	7	5	3	2	5	4	2	2	2	2
<i>wt %</i>												
SiO <sub>2</sub>	40.74	39.23	40.33	39.69	39.35	39.26	39.07	39.94	39.19	39.25	38.48	38.81
TiO <sub>2</sub>	0.00	0.02	0.01	0.01	0.01	0.03	0.02	0.01	0.03	0.02	0.04	0.03
Al <sub>2</sub> O <sub>3</sub>	0.00	0.03	0.02	0.12	0.05	0.04	0.05	0.02	0.03	0.03	0.02	0.03
Cr <sub>2</sub> O <sub>3</sub>	0.01	0.03	0.02	0.13	0.05	0.06	0.01	0.03	0.02	0.00	0.01	0.01
FeO	8.94	15.33	11.45	13.90	15.59	16.51	16.12	13.12	17.39	17.07	17.83	16.84
MnO	0.17	0.26	0.23	0.23	0.35	0.40	0.26	0.27	0.35	0.28	0.20	0.28
NiO	0.44	0.16	0.29	0.33	0.15	0.25	0.26	0.31	0.00	0.00	0.05	0.03
MgO	50.25	44.47	47.88	45.70	44.11	43.47	43.90	46.48	42.30	43.03	42.62	43.25
CaO	0.03	0.34	0.13	0.23	0.26	0.27	0.23	0.19	0.69	0.36	0.37	0.38
Na <sub>2</sub> O	0.01	0.01	0.01	0.02	0.02	0.01	0.01	0.02	0.02	0.01	0.02	0.02
K <sub>2</sub> O	0.01	0.00	0.00	0.01	0.01	0.01	0.00	0.01	0.00	0.00	0.01	0.00
Total	100.59	99.89	100.38	100.38	99.95	100.30	99.93	100.41	100.02	100.04	99.64	99.67
<i>Formula proportions based on 3 cations and 4 oxygen atoms</i>												
Si	0.991	0.990	1.062	0.991	0.994	0.993	0.990	0.993	1.00	0.996	0.986	0.989
Ti	0.000	0.000	0.000	0.000	0.000	0.001	0.000	0.000	0.00	0.000	0.001	0.000
Al	0.000	0.001	0.001	0.004	0.001	0.001	0.001	0.001	0.00	0.001	0.001	0.001
Cr	0.000	0.001	0.000	0.003	0.001	0.001	0.000	0.001	0.00	0.000	0.000	0.000
Fe	0.182	0.324	0.214	0.291	0.332	0.354	0.343	0.276	0.37	0.362	0.382	0.359
Mn	0.003	0.006	0.005	0.005	0.008	0.009	0.006	0.006	0.01	0.006	0.004	0.006
Ni	0.009	0.003	0.006	0.007	0.003	0.005	0.005	0.006	0.00	0.000	0.001	0.001
Mg	1.822	1.674	1.881	1.699	1.658	1.634	1.656	1.718	1.60	1.628	1.628	1.643
Ca	0.001	0.009	0.004	0.006	0.007	0.007	0.006	0.005	0.02	0.010	0.010	0.010
<i>mg-no.</i>	91	84	89	85	83	82	83	86	81	82	81	82

Microprobe analyses obtained using a CAMECA SX 51 electron microprobe wavelength-dispersive system (University of Heidelberg). Operating conditions were 20 nA beam current and 15 kV accelerating voltage. *mg*-number = 100[atomic Mg/(Mg + Fe<sup>2+</sup>)].

(Fig. 3) are small for the more primitive samples (*mg*-number >50) from Barmer, Bhuj and Mundwara, a feature consistent with crystal fractionation involving predominantly olivine and clinopyroxene. In contrast, the more differentiated samples from Barmer and Mundwara exhibit large variations in the abundances of Rb and Zr, a feature difficult to reconcile with closed-system crystal fractionation. It is also clear from Fig. 3 that the samples from the Deccan alkaline complexes contain higher absolute Rb contents compared with the Réunion samples for similar *mg*-numbers.

Primitive mantle-normalized patterns for the average contents of trace elements for the least differentiated samples (*mg*-number >50) from each of the alkaline complexes are shown in Fig. 4. Also included are normalized patterns for primitive olivine basalts from the

oceanite series, Réunion (Fisk *et al.*, 1988), and for N-MORB (Sun & McDonough, 1989). Important points to note from Fig. 4 are: (1) all the alkaline, silica-undersaturated samples show enrichment in highly incompatible trace elements, consistent with an origin via small degrees of partial melting; (2) the patterns for the most primitive samples from Bhuj, Barmer and Mundwara are fairly similar, with the level of enrichment correlating positively with the degree of alkalinity (undersaturation); (3) all patterns are anchored at similar Y-normalized values.

#### Nd, Sr and Pb isotopic data

For all complexes, only the most primitive samples (*mg*-number >50) were selected for isotopic analysis, and

Table 3: Representative average microprobe analyses of clinopyroxene phenocrysts for samples from Bhuj, Barmer and Mundwara

Sample:	95-Bhuj-016						95-BMR-037						95-MUN-028	
Grain no.:	1	2	3	4	5	6	1	2	3	4	5	6	1	2
No. of analyses:	26	6	4	7	5	4	14	10	13	11	12	10	9	27
<i>wt %</i>														
SiO <sub>2</sub>	46.39	46.59	46.54	45.84	46.92	46.41	47.60	47.42	46.56	47.12	48.45	46.92	49.70	49.08
TiO <sub>2</sub>	2.55	2.54	2.66	2.82	2.22	2.52	2.43	2.54	2.67	2.69	1.94	2.49	2.00	2.19
Al <sub>2</sub> O <sub>3</sub>	6.41	6.41	6.33	6.77	6.10	6.36	5.72	5.55	6.32	5.66	5.54	5.90	3.84	4.32
Cr <sub>2</sub> O <sub>3</sub>	0.35	0.34	0.42	0.39	0.68	0.36	0.10	0.05	0.38	0.04	0.09	0.02	0.02	0.03
Fe <sub>2</sub> O <sub>3</sub>	4.11	3.84	3.97	4.36	4.04	4.58	4.08	3.81	4.04	3.96	3.28	4.54	3.12	3.34
FeO	2.58	2.84	2.75	2.52	2.13	2.38	2.14	2.16	2.25	2.51	2.82	2.54	4.38	3.92
MnO	0.10	0.10	0.10	0.08	0.10	0.09	0.08	0.07	0.06	0.07	0.09	0.08	0.24	0.24
MgO	13.11	13.12	13.27	12.96	13.58	13.31	14.12	14.07	13.56	13.55	14.20	13.31	13.29	13.39
CaO	23.33	23.24	23.23	23.24	23.25	23.32	22.50	22.86	22.40	23.25	22.16	22.72	22.58	22.55
Na <sub>2</sub> O	0.40	0.40	0.38	0.40	0.41	0.36	0.62	0.50	0.62	0.48	0.66	0.62	0.85	0.80
Total	99.34	99.42	99.66	99.37	99.42	99.70	99.40	99.05	98.86	99.32	99.22	99.13	100.04	99.87
<i>Formula proportions* based on 4 cations and 6 oxygen atoms</i>														
Si	1.737	1.742	1.737	1.717	1.751	1.732	1.770	1.770	1.744	1.761	1.801	1.758	1.847	1.826
Al <sup>IV</sup>	0.263	0.258	0.263	0.283	0.249	0.268	0.230	0.230	0.256	0.239	0.199	0.242	0.153	0.174
Al <sup>VI</sup>	0.021	0.025	0.016	0.017	0.020	0.012	0.021	0.015	0.024	0.011	0.044	0.019	0.015	0.016
Ti	0.072	0.072	0.075	0.080	0.062	0.071	0.068	0.072	0.076	0.076	0.054	0.070	0.056	0.061
Cr	0.010	0.010	0.012	0.011	0.020	0.011	0.003	0.001	0.011	0.001	0.003	0.001	0.001	0.001
Fe <sup>3+</sup>	0.116	0.108	0.112	0.123	0.114	0.129	0.115	0.107	0.114	0.111	0.092	0.128	0.087	0.094
Fe <sup>2+</sup>	0.081	0.089	0.086	0.079	0.066	0.074	0.066	0.067	0.071	0.079	0.087	0.079	0.136	0.122
Mn	0.003	0.003	0.003	0.002	0.003	0.003	0.003	0.002	0.002	0.002	0.003	0.003	0.008	0.007
Mg	0.732	0.732	0.738	0.724	0.755	0.741	0.782	0.782	0.757	0.755	0.786	0.743	0.736	0.742
Ca	0.936	0.932	0.930	0.934	0.930	0.933	0.897	0.915	0.900	0.931	0.883	0.912	0.899	0.899
Na	0.029	0.029	0.027	0.029	0.029	0.026	0.044	0.036	0.045	0.035	0.048	0.045	0.061	0.058
<i>mg-no.</i>	90	89	89	90	92	91	92	92	91	91	90	90	84	86
Wo	0.501	0.500	0.497	0.501	0.498	0.496	0.482	0.488	0.488	0.496	0.477	0.489	0.482	0.482
Fs	0.107	0.107	0.108	0.110	0.098	0.110	0.099	0.095	0.101	0.102	0.098	0.113	0.124	0.120
En	0.392	0.393	0.395	0.389	0.404	0.394	0.420	0.417	0.410	0.402	0.425	0.398	0.394	0.398

See Table 2 footnote. Compositions are expressed as molar end-members Wo (Ca cation proportions), Fs (Fe<sup>2+</sup> + Fe<sup>3+</sup> + Mn cation proportions), and En (Mg cation proportions). *mg-number* = 100[atomic Mg/(Mg + Fe<sup>2+</sup>)].

\*Fe<sup>3+</sup> content was calculated stoichiometrically.

results are listed in Tables 5 (Nd and Sr) and 6 (Pb). Initial <sup>87</sup>Sr/<sup>86</sup>Sr, <sup>143</sup>Nd/<sup>144</sup>Nd and Pb isotope ratios were calculated assuming an emplacement age of ~65 Ma. Given the extremely high abundances of Sr (~2400 to >3 × 10<sup>4</sup> ppm) for the carbonatites (Table 3), and the relatively young age of the complexes, their measured <sup>87</sup>Sr/<sup>86</sup>Sr ratios are considered to approximate initial values.

Compared with the initial Sr and Nd isotope ratios for all samples (Table 3), the basanite–nephelinites from

Bhuj contain the lowest initial <sup>87</sup>Sr/<sup>86</sup>Sr (0.70357–0.70396) and highest initial <sup>143</sup>Nd/<sup>144</sup>Nd (0.51281–0.51287) ratios. In a plot of initial <sup>87</sup>Sr/<sup>86</sup>Sr vs initial <sup>143</sup>Nd/<sup>144</sup>Nd ratios (Fig. 5), the samples from Bhuj fall between the fields defined for present-day Indian MORB and that representing the composition of Réunion ‘plume’ mantle at ~65 Ma (Dupré & Allègre, 1983; Fisk *et al.*, 1988). The melilitites from Barmer also fall within the ‘depleted’ quadrant of Fig. 5, but contain more radiogenic Sr and lower Nd isotope values compared with the

Table 4: Major and trace element data

Sample:	95-AMDO-001	95-AMDO-002	95-BHUJ-016	95-BHUJ-017	95-BHUJ-018	95-BHUJ-019	95-MUN-021	95-MUN-025	95-MUN-028	95-MUN-029	95-MUN-030	95-MUN-031	95-MUN-034
Type:	BN	C	BN	BN	BN	BN	T	T-P	I	NS	P-N	T	N-B
<i>Major elements (wt%)</i>													
SiO <sub>2</sub>	49.10	12.93	40.90	42.07	42.26	42.20	47.46	52.39	41.21	53.05	51.72	43.46	40.90
TiO <sub>2</sub>	2.24	0.17	2.64	2.60	3.48	3.63	3.06	1.89	5.60	1.04	1.41	4.77	5.81
Al <sub>2</sub> O <sub>3</sub>	13.46	0.06	11.50	12.07	12.56	13.31	17.37	17.78	12.63	21.71	19.33	11.57	11.91
Fe <sub>2</sub> O <sub>3</sub>	14.39	5.39	13.40	14.01	14.84	15.32	10.07	7.79	13.79	4.11	6.12	14.94	15.38
MnO	0.21	0.55	0.22	0.20	0.20	0.19	0.26	0.19	0.25	0.13	0.18	0.27	0.23
MgO	6.54	0.39	13.40	12.69	11.45	9.08	3.09	2.28	8.32	0.76	1.42	7.13	7.90
CaO	11.64	44.17	12.10	10.77	10.96	9.83	7.50	4.38	11.12	2.25	3.19	12.20	12.55
Na <sub>2</sub> O	2.19	0.11	3.16	3.38	2.17	3.56	5.08	7.57	3.89	9.28	8.50	2.95	2.98
K <sub>2</sub> O	0.29	0.00	0.91	1.16	1.65	0.97	2.30	4.29	2.20	5.43	4.70	1.58	1.72
P <sub>2</sub> O <sub>5</sub>	0.19	1.58	0.77	0.47	0.37	0.45	0.74	0.50	1.10	0.22	0.42	0.63	0.71
LOI	0.67	—	0.97	0.76	0.60	2.33	2.91	0.69	0.46	1.46	2.79	1.51	1.25
Total	100.98	65.35	100.00	100.32	100.64	100.95	99.87	99.77	100.65	99.46	99.80	101.08	101.39
mg-no.	53	—	71	69	66	59	43	42	60	31	36	54	56
<i>Trace elements (ppm)</i>													
Ce	40	3522	118	85	68	73	243	217	277	167	182	151	177
Cr	347	—	995	943	681	429	<d/l	32	551	<d/l	18	359	264
Ni	109	—	332	312	220	168	<d/l	18	113	3	3	96	92
Sc	36	—	36	26	28	16	12	<d/l	27	<d/l	<d/l	46	27
Zn	155	—	137	140	135	157	188	175	190	121	164	174	183
Ga	21	—	14	18	19	19	29	29	24	25	32	22	23
Nb	8	360	47	37	34	34	186	181	197	180	197	98	110
Rb	7.6	—	32.3	31.9	43.6	43.4	93.4	164	66.3	142	161	58.5	48.9
Sr	202	2409	647	659	629	631	1377	1291	1635	1758	1420	785	890
Y	31	176	26	23	22	22	46	24	48	15	20	29	33
Zr	126	46	112	184	174	174	592	837	524	433	979	319	371
Cl	100	—	<d/l	200	100	100	<d/l	3200	1100	4000	3300	100	500
F	<d/l	—	200	<d/l	<d/l	<d/l	1900	1000	1000	600	700	<d/l	300

samples from Bhuj. In addition, the melilitites from Barmer contain similar initial  $^{87}\text{Sr}/^{86}\text{Sr}$  ratios but slightly lower initial  $^{143}\text{Nd}/^{144}\text{Nd}$  ratios compared with the composition of the Réunion plume (Fig. 5). Figure 5 also clearly shows that the initial  $^{143}\text{Nd}/^{144}\text{Nd}$  ratios for the carbonatites and melilitites from Barmer do not entirely overlap, with the former having slightly lower values. This feature suggests that the carbonatite and associated silicate rocks from Barmer do not share a common melt evolutionary history, and/or derivation from an isotopically heterogeneous mantle. This result is consistent with similar findings based on isotope results from previous investigations of several East African carbonatite complexes (e.g. Napak, Uganda—Simonetti & Bell, 1994a; Chilwa Island, Malawi—Simonetti & Bell, 1994b;

Mount Elgon, Uganda—Simonetti & Bell, 1995; Oidoinyo Lengai, Tanzania—Bell & Dawson, 1995; Bell & Simonetti, 1996). Also shown in Fig. 5 are the initial Sr and Nd isotope data for nephelinites and phonolites from Mundwara, and these plot at higher initial Sr but similar initial Nd isotope ratios compared with those for samples from Barmer. In addition, initial Nd and Sr isotope ratios for most of the samples from Barmer and Mundwara (Fig. 5) cluster at the ‘depleted’ end of the isotopic array defined by data for picritic and basaltic lavas from the northwestern Deccan Traps region (Peng & Mahoney, 1995; locations shown in Fig. 1). This array was interpreted as representing mixing between mantle end-members similar in composition to that of Réunion and continental lithosphere (Peng & Mahoney, 1995). In the

Table 4: continued

Sample:	95-BMR-036	95-BMR-037	95-BMR-038	95-BMR-039	95-BMR-039	95-BMR-045	95-BMR-046	95-BMR-047	95-BMR-048	95-BMR-054	95-BMR-055	95-BMR-056
Type:	M	M	M	M	P-N	P	P	P	P	C	C	C
<i>Major elements (wt %)</i>												
SiO <sub>2</sub>	35.32	36.90	36.43	36.70	47.58	55.67	52.43	52.51	52.33	1.29	2.12	0.66
TiO <sub>2</sub>	6.20	5.82	6.05	6.04	1.19	0.41	0.43	0.37	0.29	0.04	0.10	0.05
Al <sub>2</sub> O <sub>3</sub>	10.73	10.95	10.93	11.01	16.70	21.67	19.84	19.77	21.45	0.14	0.32	0.06
Fe <sub>2</sub> O <sub>3</sub>	16.89	15.96	16.92	17.08	7.26	3.34	5.06	4.88	3.71	1.60	2.24	2.07
MnO	0.22	0.20	0.20	0.21	0.40	0.30	0.26	0.26	0.29	2.00	2.11	2.70
MgO	7.93	9.93	9.55	8.73	1.39	0.20	0.20	0.13	0.05	0.21	0.91	1.33
CaO	16.55	14.13	15.34	15.62	8.20	0.80	1.99	1.92	0.97	31.05	30.39	28.12
Na <sub>2</sub> O	2.77	2.79	3.02	3.23	8.10	11.16	10.60	10.18	12.11	1.42	0.72	0.76
K <sub>2</sub> O	1.32	2.16	1.97	1.64	4.05	5.19	6.34	7.17	5.13	0.03	0.21	0.04
P <sub>2</sub> O <sub>5</sub>	0.77	0.68	0.70	0.75	0.48	0.05	0.06	0.06	0.03	0.10	0.45	0.07
LOI	2.51	1.41	0.10	0.46	3.37	1.26	2.33	1.99	3.23	—	—	—
Total	101.24	101.02	101.28	101.52	98.75	100.07	99.56	99.27	99.62	37.85	39.57	35.87
mg-no.	54	61	58	56	32	13	9	6	3			
<i>Trace elements (ppm)</i>												
Ce	183	120	142	150	548	182	202	188	201	54810	45765	53838
Cr	31	573	419	233	16	<d/l	<d/l	<d/l	<d/l	—	—	—
Ni	26	103	73	59	7	<d/l	3	4	<d/l	—	—	—
Sc	51	41	54	51	12	<d/l	<d/l	<d/l	<d/l	—	—	—
Zn	162	147	151	155	217	196	236	237	230	—	—	—
Ga	22	21	21	23	21	36	35	35	34	—	—	—
Nb	107	89	94	102	292	333	154	172	260	43	423	18
Rb	41.9	63.2	54.5	46.1	100	155	219	237	170	—	—	—
Sr	1357	789	859	909	4598	642	1875	1938	1005	33678	31426	30079
Y	29	25	26	28	44	19	10	9	22	108	128	116
Zr	355	287	307	328	767	1068	618	626	963	1169	1524	1598
Cl	100	100	100	<d/l	2300	300	3400	5000	1800	—	—	—
F	<d/l	100	<d/l	200	1100	1600	2400	2300	2200	—	—	—

Analyses obtained from geochemical laboratories, McGill University, using a Philips PW2400 automated XRF spectrometer. Analysis of major and certain trace elements (Ce, Cr, Ni, Zn) obtained from fused beads prepared from ignited samples (using a 1:5 ratio of sample to lithium tetraborate). Remaining trace elements were determined from pressed pellets. Accuracy for SiO<sub>2</sub> and other major elements is  $\pm 0.5\%$  and 1% of quoted value, respectively. For trace elements, the accuracy is within 5% of the quoted value. Detection limits for most trace elements is  $\sim 1$  ppm, except for Ce (15 ppm), Cl (100 ppm), Cr (15 ppm), F (100 ppm), Ni (3 ppm), Zn (2 ppm). Rock type: BN, basanite; C, carbonatite; I, ijolite; M, melilitite; T, tephrite; T-P, tephri-phonolite; N-B, nephelinite-basanite; NS, nepheline syenite; P, phonolite; P-N, phonolitic nephelinite. —, not analysed; <d/l, below detection limit. *mg*-number =  $100[\text{atomic Mg}/(\text{Mg} + \text{Fe}^{2+})]$  assuming  $\text{Fe}_2\text{O}_3/\text{FeO} = 0.20$ .

lower right quadrant of Fig. 5, the initial Nd and Sr isotope ratios for carbonatite dyke 95-AMDO-002 plot within the previously established field for Amba Dongar (Simonetti *et al.*, 1995). In contrast, the initial Nd and Sr isotope ratios for the basanite from the central plug at Amba Dongar plot close to the Réunion field, and are distinct from those for the surrounding carbonatite (Fig. 5). The isotope systematics for carbonatite and adjacent basanite at Amba Dongar are not uniform, a

finding also observed for Barmer and other alkaline complexes world wide.

Present-day Pb isotope ratios for carbonatite are considered to approximate initial ratios because of the relatively young age of the complexes ( $\sim 65$  Ma), and the generally low U/Pb and Th/Pb ratios characteristic of carbonatites (e.g. Grünenfelder *et al.*, 1986; Nelson *et al.*, 1988; Kwon *et al.*, 1989; also for natrocarbonatites—Simonetti *et al.*, 1997; this study, Table 6). A plot of

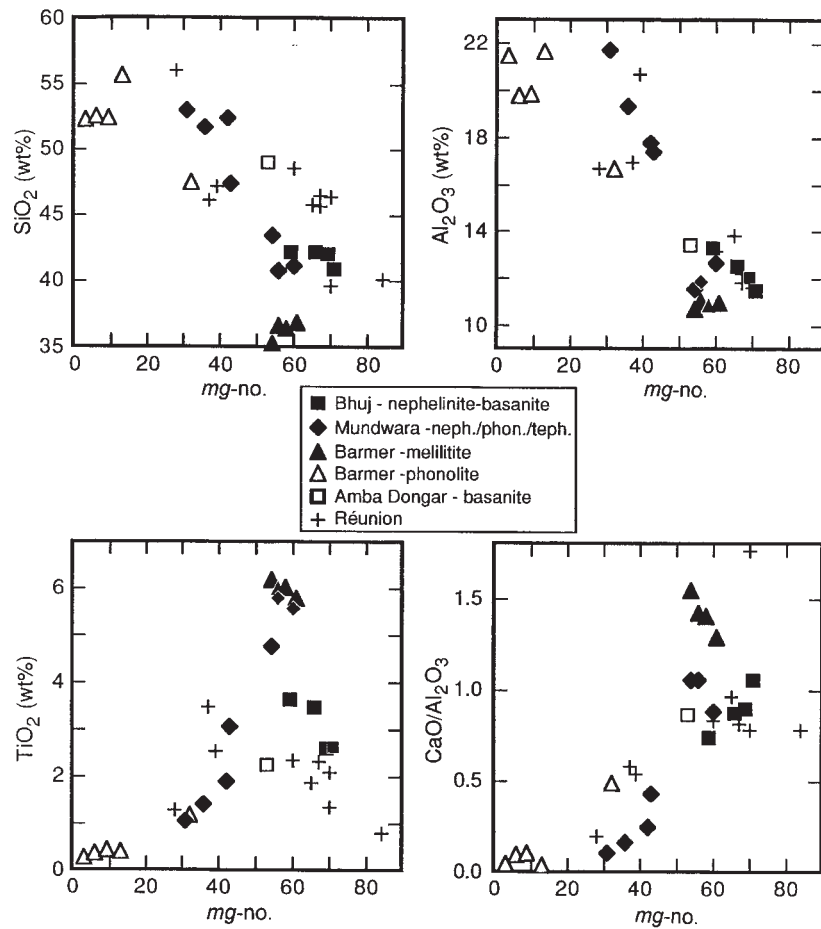


**Fig. 2.** Selected major element variations vs *mg*-number for samples listed in Table 4. Data for Réunion volcanics (primitive shield phase and differentiated series) from Fisk *et al.* (1988).

initial <sup>206</sup>Pb/<sup>204</sup>Pb vs initial <sup>207</sup>Pb/<sup>204</sup>Pb (Fig. 6) shows the data listed in Table 6, in addition to the fields for Indian MORB, the Réunion plume component (Oversby, 1972), the carbonatites from Amba Dongar (Simonetti *et al.*, 1995), and both arrays defined by picrites and basaltic lavas from the northwestern Deccan province (Peng & Mahoney, 1995). As in the case for their initial Nd and Sr isotope data (Fig. 5), the basanite–nephelinites from Bhuj contain initial Pb isotope ratios that plot between the Réunion and Indian MORB fields (Fig. 6). The initial Pb isotope ratios for samples from Bhuj and basanite from Amba Dongar are clearly less radiogenic compared with the remaining samples (Fig. 6). Data for carbonatites and mellilitites from Barmer shown in Fig. 6 are similar (with the exception of sample 95-BMR-038, Table 6), and fall very close to the Réunion field. Initial Pb isotope ratios for the Mundwara nephelinites overlap those for the samples from Barmer (Fig. 6). Carbonatite sample

95-AMDO-001 contains initial Pb isotope ratios that plot within the field previously defined for Amba Dongar carbonatites (Simonetti *et al.*, 1995). A noteworthy feature of Fig. 6 is that the initial Pb isotope ratios for most of the samples from Barmer, Mundwara, and Amba Dongar form a near-vertical array and overlap one of the trends (1) defined by the mildly alkaline picritic and basaltic Deccan lavas from Peng & Mahoney (1995).

With the exception of the samples from Bhuj, the various silicate rock types from the Deccan alkaline complexes share several characteristics. These include having approximately the same level of incompatible trace element enrichment and similar primitive mantle-normalized patterns (Fig. 4). The large variation in the initial Nd, Pb, and Sr isotope ratios for the least differentiated rock types from the individual complexes, however, are clearly indicative of derivation from isotopically distinct mantle sources.

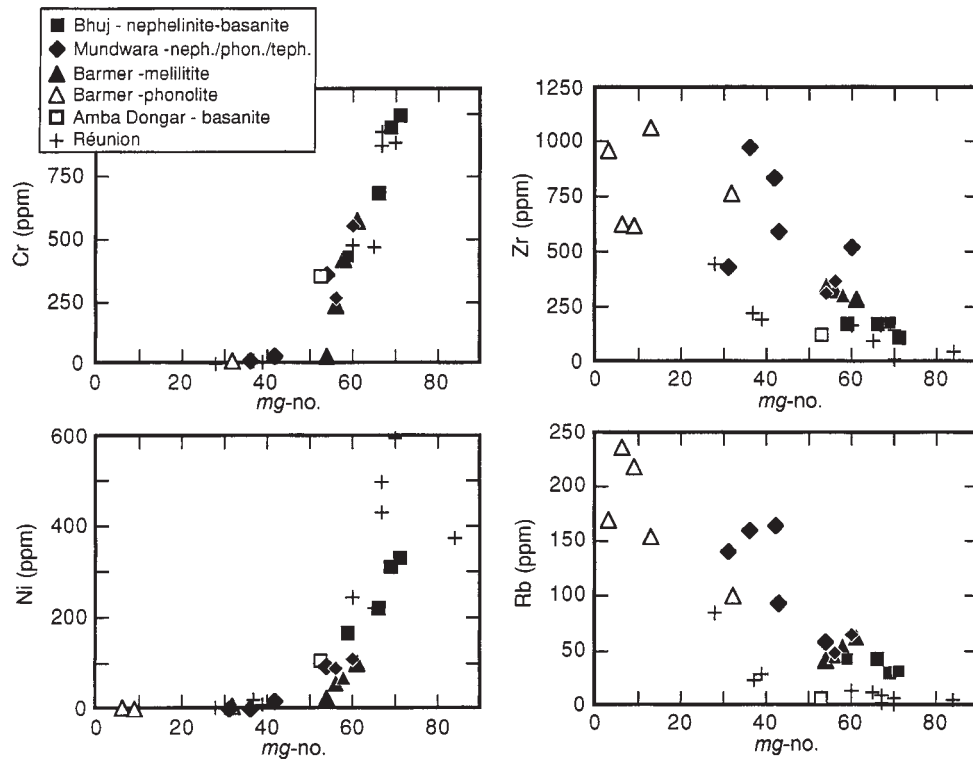


Fig. 3. Selected trace element variations vs *mg*-number for samples listed in Table 4. Data for Réunion volcanics (primitive shield phase and differentiated series) from Fisk *et al.* (1988).

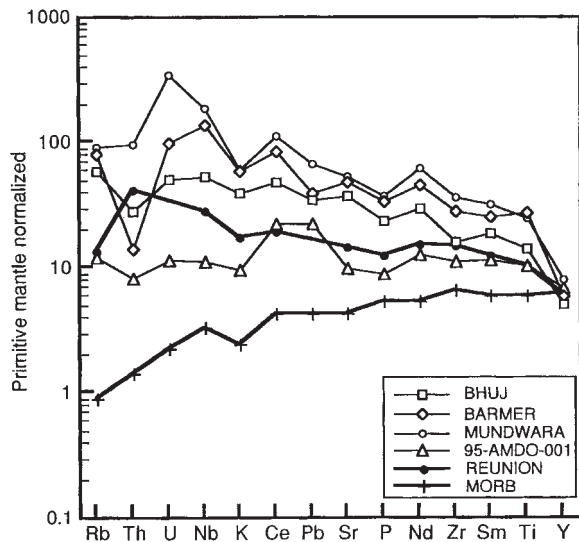


Fig. 4. Primitive mantle-normalized diagram showing patterns for average trace element compositions for the least differentiated (*mg*-number >50) silicate samples from Amba Dongar, Barmer, Bhuj, and Mundwara (concentrations from Tables 4–6). Data for MORB and primitive mantle, and for Réunion taken from Sun & McDonough (1989) and Fisk *et al.* (1988), respectively.

## DISCUSSION

### Mantle sources

Compared with the initial Nd and Sr isotope ratios from Amba Dongar and Mundwara, the complexes of Bhuj and Barmer are characterized by lower initial  $^{87}\text{Sr}/^{86}\text{Sr}$  and higher initial  $^{143}\text{Nd}/^{144}\text{Nd}$  ratios, and these correspond more closely to those for Réunion mantle (Fig. 5). Basu *et al.* (1993) reported initial Sr isotope and  $^3\text{He}/^4\text{HeRA}$  ratios (from clinopyroxene) (where *RA* is the air ratio) for pyroxenite and gabbro from the complexes of Mundwara, Sarnu (Barmer) and Phenai Mata. More importantly, the range in observed  $^3\text{He}/^4\text{HeRA}$  ratios for the slightly older complexes of Mundwara (8.5–13.9), and Barmer (12.4–12.8) are similar to the  $^3\text{He}/^4\text{HeRA}$  value of 14 measured for the Réunion hotspot (Craig & Rison, 1982; Graham *et al.*, 1990). The He isotope data provide, therefore, evidence for the participation of Réunion plume mantle in the derivation, at the very least, of the slightly older (northern) Deccan alkaline complexes (Basu *et al.*, 1993).

With the exception of the carbonatites from Amba Dongar, the initial  $^{143}\text{Nd}/^{144}\text{Nd}$  and  $^{87}\text{Sr}/^{86}\text{Sr}$  isotope values from the remaining complexes plot either close to (Bhuj) or at slightly lower Nd isotope ratios compared with that for Réunion mantle (Fig. 5). In addition, the

Table 5: Nd and Sr isotope data

Sample	Rock type	Rb (ppm)*	Sr (ppm)	<sup>87</sup> Rb/ <sup>86</sup> Sr	<sup>87</sup> Sr/ <sup>86</sup> Sr measured	<sup>87</sup> Sr/ <sup>86</sup> Sr initial	Nd (ppm)	Sm (ppm)	<sup>147</sup> Sm/ <sup>144</sup> Nd	<sup>143</sup> Nd/ <sup>144</sup> Nd measured	<sup>143</sup> Nd/ <sup>144</sup> Nd initial
<i>Amba Dongar</i>											
95-AMDO-001	BN	7.6	209.2	0.1025	0.704569	0.704474	17.4	5.1	0.1756	0.512877	0.512802
95-AMDO-002	C		2409*		0.705530	0.705530†	987.3	120	0.0734	0.512558	0.512527
<i>Bhuj</i>											
95-BHUJ-016	BN	32.3	1046	0.0871	0.703834	0.703754	59.9	11.9	0.1201	0.512864	0.512813
95-BHUJ-017	BN	31.9	735.3	0.1224	0.703679	0.703566	37.3	7.8	0.1258	0.512918	0.512865
95-BHUJ-018	BN	43.6	668.5	0.1840	0.704130	0.703960	30.6	6.7	0.1315	0.512880	0.512824
95-BHUJ-019	BN	43.4	722.4	0.1695	0.703740	0.703583	34.9	7.2	0.1252	0.512911	0.512858
<i>Barmer</i>											
95-BMR-036	M	41.9	1357	0.0871	0.704335	0.704255	42.7	7.3	0.1036	0.512762	0.512718
95-BMR-037	M	63.2	836.4	0.2132	0.704529	0.704332	64.1	11.8	0.1110	0.512802	0.512755
95-BMR-038	M	54.5	911.6	0.1687	0.704416	0.704260	68.1	12.5	0.1109	0.512818	0.512771
95-BMR-039	M	46.1	978.6	0.1329	0.704376	0.704253	72.4	13.2	0.1106	0.512817	0.512770
95-BMR-054	C		33678*		0.704262	0.704262†	7283	422	0.0350	0.512717	0.512702
95-BMR-055	C		31426*		0.704305	0.704305†	5786	339	0.0354	0.512724	0.512709
95-BMR-056	C		30079*		0.704227	0.704227†	9316	566	0.0368	0.512679	0.512663
<i>Mundwara</i>											
95-MUN-021	T	93.4	1377	0.1913	0.705872	0.705695	96.5	16.7	0.1047	0.512764	0.512720
95-MUN-028	I	66.3	1635	0.1144	0.704786	0.704680	110.6	18.1	0.0991	0.512797	0.512755
95-MUN-030	P-N	160.5	1442	0.3140	0.704902	0.704612	50.8	7.7	0.0921	0.512773	0.512734
95-MUN-031	T	58.5	831.3	0.1985	0.704965	0.704782	64.9	11.5	0.1071	0.512793	0.512747
95-MUN-034	N-B	48.9	951.9	0.1449	0.704680	0.704546	76.3	13.6	0.1078	0.512738	0.512692

Isotope ratios normalized to  $^{146}\text{Nd}/^{144}\text{Nd} = 0.7219$  and  $^{86}\text{Sr}/^{88}\text{Sr} = 0.1194$ . Repeated analyses of standards yielded averages of  $0.710245 \pm 0.000018$  ( $2\sigma$ ,  $n = 6$ ) for NBS 987 Sr standard, and  $0.511870 \pm 0.000018$  ( $2\sigma$ ,  $n = 6$ ) for La Jolla Nd standard. Total chemistry blanks were  $<500$  pg for Sr and  $<100$  pg for Nd. Uncertainties for Nd, Sm, and Sr concentrations  $<0.5\%$ . Rock type: BN, basanite; C, carbonatite; I, ijolite; M, melilitite; T, tephrite; N-B, nephelinite-basanite; P-N, phonolitic nephelinite. \*Rb concentrations for all samples and Sr abundances for carbonatites are from XRF analyses (see Table 2). Initial ratios were calculated assuming an age of 65 Ma.

†For carbonatite samples, measured Sr isotope ratios approximate initial values.

initial Pb isotope data for most of the samples studied here plot close to the composition of Réunion mantle (Fig. 6). The Nd, Pb and Sr isotope data for samples from Barmer, Mundwara and Amba Dongar also overlap those for mildly alkaline picrites and basaltic lavas from the northwestern Deccan flows (trend 1, Peng & Mahoney, 1995). The latter define near-vertical arrays in Pb–Pb isotope diagrams (Fig. 6) and an Nd–Sr isotope array (Fig. 5), which were both attributed to mixing between a Réunion plume mantle and continental lithosphere (Peng & Mahoney, 1995). Moreover, based on the incompatible trace element enriched nature of mildly alkaline picritic and basaltic lava flows from the northwestern Deccan (Fig. 1), Peng & Mahoney (1995) proposed that melting within the upper mantle occurred at greater average depths and over a shorter depth interval

for these basalts than for their counterparts located in the southern part of the province. The data shown in Figs 5 and 6 suggest, therefore, that continental lithosphere played an important role in the generation of Deccan alkaline magmatism. The isotope results shown in Figs 5–7 clearly indicate, however, that a third end-member is required to explain the variation in the isotopic data. The most likely candidate is asthenospheric, Indian MORB-type mantle because of its isotopic similarities to the basanite–nephelinites from Bhuj. Experimental results indicate that entrainment of ambient mantle during the ascent of thermal plumes is possible because of coupling between heat conduction and laminar stirring driven by plume motion (Griffiths & Campbell, 1990). On the basis of results from recent numerical models investigating the role of thermal entrainment and melting in mantle

Table 6: Pb isotope data

Sample	Pb (ppm)	U (ppm)	Th (ppm)	<sup>206</sup> Pb/ <sup>204</sup> Pb	<sup>207</sup> Pb/ <sup>204</sup> Pb	<sup>208</sup> Pb/ <sup>204</sup> Pb	<sup>206</sup> Pb/ <sup>204</sup> Pb	<sup>207</sup> Pb/ <sup>204</sup> Pb	<sup>208</sup> Pb/ <sup>204</sup> Pb
				measured	measured	measured	initial*	initial*	initial*
95-AMD-001	001.6	0.24	0.7	18.145	15.546	38.600	18.03	15.54	38.49
95-AMD-002	67.9	2.1	30.6	19.159	15.800	40.075	19.14	15.80	39.96
95-BHUJ-016	3.2	1.7	2.8	18.868	15.586	38.921	18.48	15.57	38.71
95-BHUJ-017	2.3	1.0	3.2	18.479	15.491	38.529	18.16	15.48	38.20
95-BHUJ-018	1.9	0.7	1.7	18.642	15.497	38.613	18.38	15.49	38.40
95-BHUJ-019	2.3	0.9	1.8	18.653	15.542	38.851	18.36	15.53	38.66
95-BMR-037	2.4	1.8	1.2	19.582	15.669	39.793	19.01	15.64	39.67
95-BMR-038	2.2	2.0	1.1	21.265	15.701	42.070	20.55	15.67	41.96
95-BMR-039	3.7	2.4	1.8	19.547	15.598	39.591	19.06	15.58	39.48
95-BMR-054	—	1.3	—	18.983	15.636	39.311	18.98†	15.64†	39.31†
95-BMR-055	—	5.8	—	19.028	15.613	39.289	19.03†	15.61†	39.29†
95-BMR-056	282	0.5	—	19.021	15.635	39.381	19.02†	15.64†	39.38†
95-MUN-030	11.5	12.2	10.6	19.262	15.631	39.671	18.96	15.61	39.44
95-MUN-031	4.9	2.4	8.5	19.140	15.658	39.693	18.77	15.64	39.27
95-MUN-034	4.6	2.3	5.7	19.273	15.611	39.702	18.97	15.59	39.40

Procedural blanks for Pb, U and Th are 50–100, 2–6 and 80–150 pg, respectively, and considered negligible. Mass fractionation corrections of 0.09 ( $\pm 0.03$ , 2 $\sigma$ )/a.m.u. and 0.24%/a.m.u. were applied to Pb isotope ratios (based on repeated measurements of NIST SRM 981 Pb standard) using Faraday and Daly analogue detectors, respectively. Uncertainties associated with Pb, U and Th concentration determinations are <1%; —, not analysed.

\*Initial values were calculated assuming an age of 65 Ma.

†For carbonatite samples, measured Pb isotope ratios approximate initial values.

plumes, Farnetani & Richards (1995) suggested that the isotopic heterogeneity is inherent to the plume itself or the result of contamination from crust and lithosphere through which the primary magmas ascend. With regard to Réunion plume–lithosphere interaction, however, the Nd, Pb and Sr isotopic compositions for the samples from Bhuj are solely consistent with contamination by lithosphere similar in composition to Indian MORB mantle.

Correlations between isotope ratios and major and trace element data would lend support to the generation of Deccan alkaline complexes involving distinct mantle sources. First, it must be shown that initial isotopic ratios are inherited from their mantle source region, and not perturbed by secondary processes, such as crustal contamination. The data listed in Tables 4 and 5 indicate that no correlations exist between Sr and Nd contents and *mg*-number, and initial <sup>87</sup>Sr/<sup>86</sup>Sr and initial <sup>143</sup>Nd/<sup>144</sup>Nd therefore are not consistent with crustal contamination.

Figure 2 clearly shows that the melilitites from Barmer are characterized by much higher CaO/Al<sub>2</sub>O<sub>3</sub> ratios compared with the silicate rocks from the remaining Deccan alkaline complexes. According to the experimental work of Herzberg (1995), partial melting at higher pressures ( $\geq 30$  kbar) stabilizes garnet relative to

olivine and pyroxene, resulting in melt products with lower Al<sub>2</sub>O<sub>3</sub> contents and higher CaO/Al<sub>2</sub>O<sub>3</sub> ratios. In addition, the low SiO<sub>2</sub> contents, high incompatible element concentrations and steep REE patterns typical of melilitites indicate that they are the result of small-degree partial melting ( $\ll 5\%$ ) of an enriched mantle source (relative to MORB-source mantle) interpreted to be carbonated phlogopite–garnet lherzolite (e.g. Brey & Green, 1977; Maaløe *et al.*, 1992; Rogers *et al.*, 1992). The CaO-rich (up to 17 wt %) and Al<sub>2</sub>O<sub>3</sub>-poor (8–10 wt %) nature of melilitites probably reflects the role of carbonate during melting and the residual nature of garnet in the source (Wilson *et al.*, 1995). Nb/Y ratios may serve to evaluate the role of residual garnet during melting, as Y would preferentially partition into residual garnet during melting, resulting in higher Nb/Y ratios in the liquids. Figure 8 plots Nb/Y ratios against *mg*-number, Nb/Zr and initial <sup>143</sup>Nd/<sup>144</sup>Nd values for the least differentiated samples (*mg*-number >50) from the Deccan alkaline complexes. These indicate that: (1) Nb/Y ratios are constant for each individual complex in the most primitive samples and samples from Barmer and Mundwara contain higher values (3–4) than those for Bhuj and Amba Dongar (1–2); (2) there is a positive correlation with Nb/Zr values, the latter being a function of degree of partial melting (higher for smaller-degree

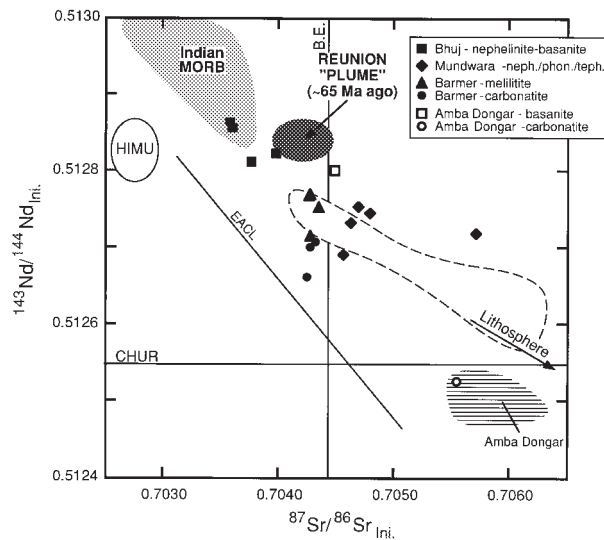


**Fig. 5.** Initial Nd vs initial Sr isotope plot containing the data from this study (Table 5), which are compared with data for Indian MORB (light grey shaded field—data taken from Cohen *et al.*, 1980; Sun, 1980; Cohen & O’Nions, 1982; Dupré & Allègre, 1983; Hamelin & Allègre, 1985; Hamelin *et al.*, 1986; Michard *et al.*, 1986; Newsom *et al.*, 1986; Price *et al.*, 1986; Ito *et al.*, 1987; Dosso *et al.*, 1988; Klein *et al.*, 1988; Mahoney *et al.*, 1989), Réunion (dark grey shaded field—data from Dupré & Allègre, 1983; Fisk *et al.*, 1988), carbonatites from Amba Dongar (horizontal striped field—data from Simonetti *et al.*, 1995), and mildly alkaline picrites and basaltic flows from northwestern Deccan (dashed field—data from Peng & Mahoney, 1995). EACL (East African Carbonatite Line) from Bell & Blenkinsop (1987*a*). Field for HIMU taken from Hart (1988). Values for lines labelled B.E. (bulk Earth) and CHUR (chondritic uniform reservoir) are those for ~65 Ma, assuming present-day values of  $^{87}\text{Sr}/^{86}\text{Sr}_{\text{BE}} = 0.7045$  and  $^{87}\text{Rb}/^{86}\text{Sr}_{\text{BE}} = 0.083$  ( $\lambda = 1.42 \times 10^{-11}$  per year) and  $^{143}\text{Nd}/^{144}\text{Nd}_{\text{CHUR}} = 0.512638$  and  $^{147}\text{Sm}/^{144}\text{Nd}_{\text{CHUR}} = 0.1967$  ( $\lambda = 6.54 \times 10^{-12}$  per year).

melts); (3) the high Nb/Y for the samples from Barmer and Mundwara correlate with lower initial Nd isotopic composition. In general, this correlation also seems to hold true between  $\text{CaO}/\text{Al}_2\text{O}_3$  ratios and initial Nd isotope compositions (Fig. 8). The data shown in Fig. 8 suggest that the basanite–nephelinites from Bhuj and Amba Dongar, and samples from Réunion were generated at similar mantle depths (and from similar mantle sources). Results from melting experiments indicate that all Piton des Neiges lavas may be derived from the parent magma composition for Réunion by fractional crystallization (augite  $\pm$  olivine) at pressures of ~1–5 kbar (Fisk *et al.*, 1988). In contrast, the higher  $\text{CaO}/\text{Al}_2\text{O}_3$  ratios for the melilitites from Barmer suggest an origin by small-degree partial melting at deeper levels within (plume-) metasomatized lithosphere. This interpretation is consistent with phase equilibria studies, which indicate that melilititic or nephelinitic melts are generated at pressures of 20–30 kbar (Eggler, 1974, 1978, 1989; Brey & Green, 1975, 1977; Edgar, 1987).

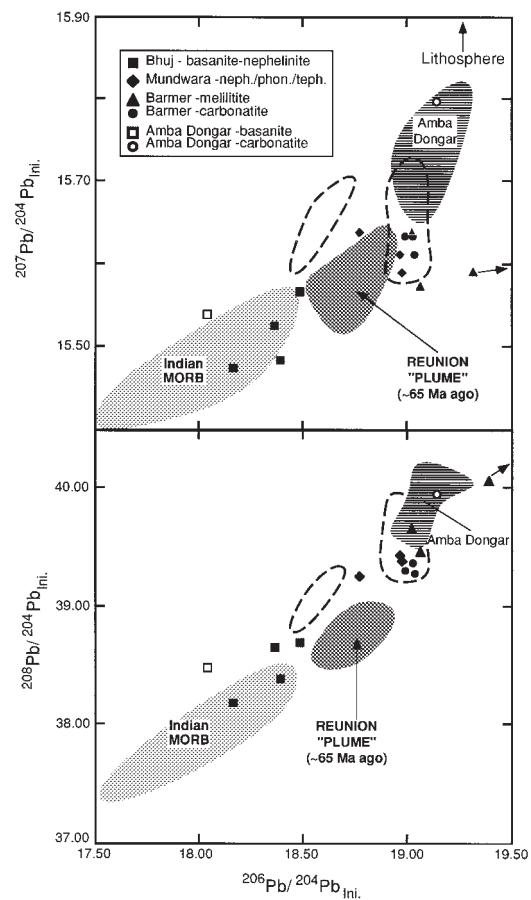


**Fig. 6.** Plots of initial  $^{206}\text{Pb}/^{204}\text{Pb}$  vs initial  $^{207}\text{Pb}/^{204}\text{Pb}$  ratios and initial  $^{208}\text{Pb}/^{204}\text{Pb}$  ratios for data listed in Table 6. Also shown for comparison are fields (same patterns as in Fig. 5) for Indian MORB (see references in caption of Fig. 5), Réunion (Oversby, 1972; Dupré & Allègre, 1983), Amba Dongar (Simonetti *et al.*, 1995), and mildly alkaline picrites and basaltic flows from northwestern Deccan (dashed field—data from Peng & Mahoney, 1995). Calculated initial Pb ratios (for ~65 Ma) for Réunion mantle are based on  $^{238}\text{U}/^{204}\text{Pb} = 10$  [refer to discussion by Peng & Mahoney (1995)], and  $\text{Th}/\text{U} = 3.3$  [from Condomines *et al.* (1988)].

### Plume–lithosphere interaction

In recent years, attempts at explaining the large variations in Nd and Sr isotope data typically exhibited by carbonatite complexes (of similar age) from individual alkaline volcanic provinces, such as the Kola Peninsula (Kola carbonatite mixing array, Kramm & Kogarko, 1994) and East Africa (e.g. Bell & Blenkinsop, 1987*a*; Bell & Simonetti, 1996; Kalt *et al.*, 1997) have included: (1) melt derivation from an isotopically heterogeneous sub-continental mantle; (2) mixing of HIMU and EMI mantle components; (3) plume–lithosphere interaction. In relation to the last, Bell & Simonetti (1996) proposed a two-stage model to explain the isotope variations shown by East African carbonatites which involved (1) release of metasomatizing agents with HIMU-like signatures

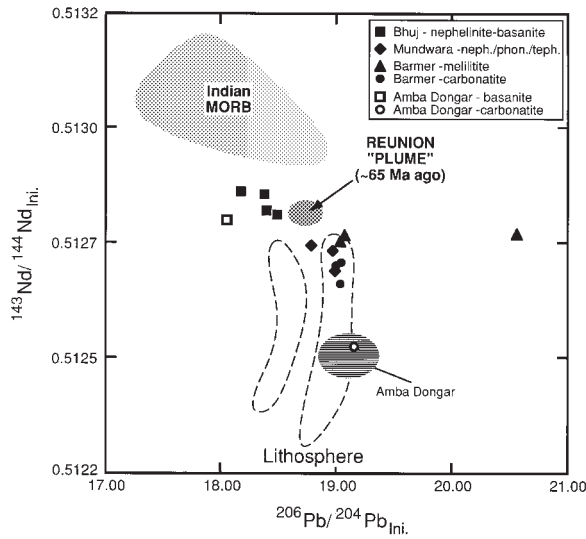


**Fig. 7.** Initial  $^{143}\text{Nd}/^{144}\text{Nd}$  vs initial  $^{206}\text{Pb}/^{204}\text{Pb}$  ratios plot for data from Deccan alkaline complexes (Tables 5 and 6). Patterns for fields and sources of data are the same as those for Figs 5 and 6.

from upwelling mantle (plume) source, which in turn metasomatize the sub-continental (EMI-like) lithosphere, and (2) variable degrees and discrete partial melting of the resulting heterogeneous, metasomatized lithosphere.

The Nd and Sr isotope data from the Deccan alkaline complexes obtained in this study are compared with the position of the East African Carbonatite Line (EACL, from Bell & Blenkinsop, 1987*a*), a line based on Nd and Sr isotope data from carbonatite complexes younger (0–30 Ma) than the Deccan alkaline complexes (Fig. 5). The Nd and Sr isotope data from the Deccan alkaline complexes are distinct from those of the East African carbonatites, and do not plot along the EACL (Fig. 5). In addition, age correction of the EACL would drive it slightly further to the lower left in Fig. 5, and this feature further eliminates the need for involving HIMU and EMI mantle components (from Hart, 1988), the proposed end-members of the EACL, in the generation of the Deccan alkaline complexes. The close similarity between the isotope data from the Deccan alkaline complexes examined here and from previous studies (e.g. Basu *et al.*, 1993) and those for present-day volcanics from Réunion supports the significant involvement of plume-type mantle

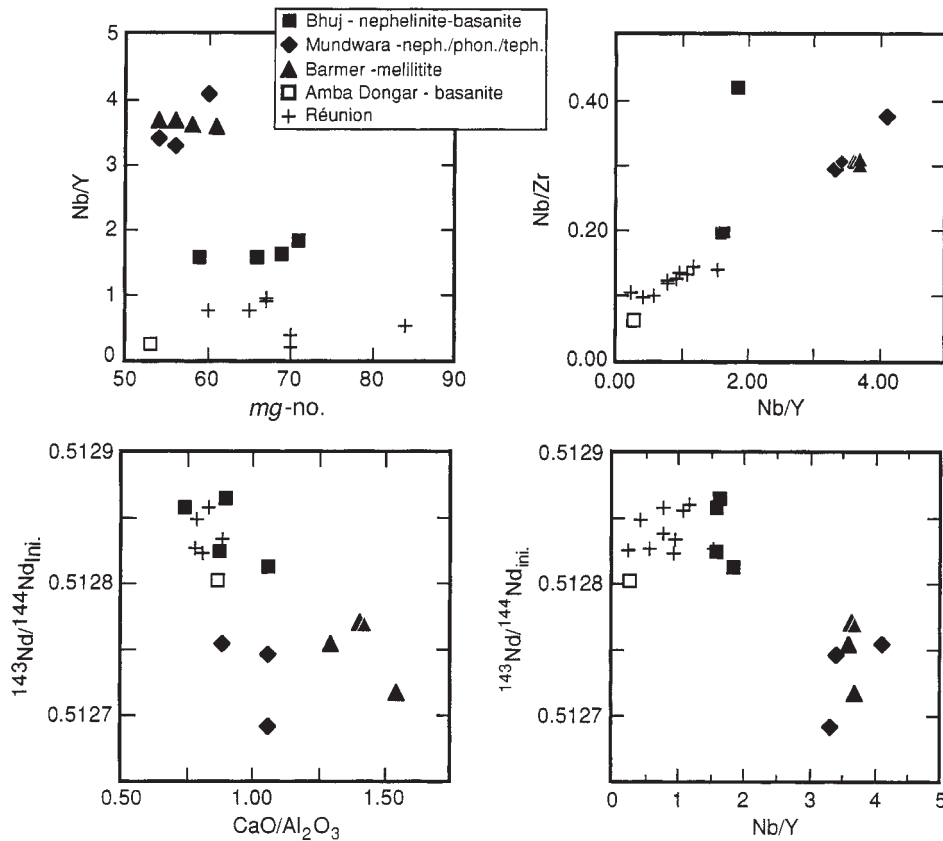


**Fig. 8.** Plots of Nb/Y vs mg-number, Nb/Zr vs Nb/Y, initial  $^{143}\text{Nd}/^{144}\text{Nd}$  ratios vs  $\text{CaO}/\text{Al}_2\text{O}_3$ , and initial  $^{143}\text{Nd}/^{144}\text{Nd}$  ratios vs Nb/Y for primitive (mg-number >50) silicate samples from Amba Dongar, Barmer, Bhuj and Mundwara. Data for Réunion taken from Fisk *et al.* (1988).

in the derivation of the former. Recent isotopic investigations of the Okenyenya igneous complex (Milner & le Roex, 1996) and Damaraland lamprophyre and carbonatite occurrences (le Roex & Lanyon, 1998) both from northwestern Namibia, which are temporally and spatially associated with the Etendeka volcanic province, also argue for the involvement of the Tristan plume in their generation. Le Roex & Lanyon (1998) have proposed a similar model for the generation of lamprophyre and carbonatite magmatism at Damaraland to the one being advocated in this study. The alkaline magmatism in northwestern Namibia is thought to be the result of melting of metasomatic vein material introduced into the sub-continental lithospheric mantle by alkaline melts or fluids derived from the upwelling Tristan mantle plume at the time of continental break-up (le Roex & Lanyon, 1998).

Based on the isotope results obtained in this study, we propose that the large variations in isotope data defined by carbonatite provinces world wide may result from the interaction between mantle perturbations or upwellings (plume component) and continental lithosphere. The excellent correlation between the temporal distribution of carbonatites and major orogenic cycles for the past 3.0 b.y. (Woolley & Kempe, 1989; Veizer *et al.*, 1993) lends support to this interpretation, a conclusion also stated by Bell & Simonetti (1996).

## CONCLUSIONS

The isotope results obtained from the least differentiated, silica-undersaturated samples from the complexes of Barmer, Bhuj, Mundwara and Amba Dongar show large variations attributable to the mixing of at least three distinct mantle end-members—asthenosphere (Indian MORB), (old) enriched continental lithosphere, and Réunion plume mantle. Correlations between major element chemistry and isotope ratios are also indicative of melt generation from distinct mantle sources. Furthermore, the isotope results obtained here are consistent with previous tectonic–petrogenetic models that propose an important contribution of Réunion plume-type mantle in the source of the alkaline complexes and Deccan lavas found in the north and northwestern regions of the province. This input may have been especially important during the early stages of plume interaction with the Indian sub-continental lithosphere. With time, and as the Indian sub-continent moved northwards over the Réunion plume, increased heating of continental lithosphere (and its consequent thinning) resulted in larger-degree partial melting and an increased input of a lithospheric isotopic ‘signal’ in subsequent production of alkaline and tholeiitic magmatism of the Deccan igneous province.

## ACKNOWLEDGEMENTS

We thank Al Hofmann, director of the Max-Planck-Institut für Chemie (MPI) für Chemie (Mainz), for his support of this project and scientific input. We thank also Hans-Peter Meyer, Mineralogisches Institut–Universität Heidelberg, for technical assistance in obtaining microprobe analyses. We are especially grateful to S. B. Vora, chief scientific officer, Research and Development, of the Gujarat Mineral Development Corporation (GMDC), for providing assistance in collecting samples, logistical support and accommodation during our stay in India. A. Simonetti acknowledges financial support of an NSERC postdoctoral fellowship. B. Ghaleb (GEOTOP) is thanked for help in obtaining U and Th isotope dilution analyses. Professor D. Francis and G. Keating, both from McGill University, are thanked for assistance in obtaining XRF analyses. Reviews by J. Davidson, T. Skulski and G. Wörner helped improve the quality of the manuscript. Comments on an earlier version of the manuscript by C. Gariépy and R. Stevenson (both at GEOTOP) are much appreciated. A. le Roex (University of Cape Town) is thanked for providing a copy of a manuscript in press.

## REFERENCES

- Baksi, A. K. (1994). Geochronological studies on whole-rock basalts, Deccan Traps, India: evolution of the timing of volcanism relative to the K–T boundary. *Earth and Planetary Science Letters* **121**, 43–56.
- Basu, A. R., Renne, P. R., DasGupta, D. K., Teichmann, F. & Poreda, R. J. (1993). Early and late alkali igneous pulses and a high-<sup>3</sup>He plume origin for the Deccan flood basalts. *Science* **261**, 902–906.
- Bell, K. & Blenkinsop, J. (1987*a*). Nd and Sr isotopic compositions of East African carbonatites: implications for mantle heterogeneity. *Geology* **15**, 99–102.
- Bell, K. & Blenkinsop, J. (1987*b*). Archean depleted mantle—evidence from Nd and Sr initial isotopic ratios of carbonatites. *Geochimica et Cosmochimica Acta* **51**, 291–298.
- Bell, K. & Dawson, J. B. (1995). Nd and Sr isotope systematics of the active carbonatite volcano, Oldoinyo Lengai. In: Bell, K. & Keller, J. (eds) *Carbonatite Volcanism: Oldoinyo Lengai and the Petrogenesis of Natrocarbonatites. IAVCEI Proceedings in Volcanology* **4**, 100–112.
- Bell, K. & Simonetti, A. (1996). Carbonatite magmatism and plume activity: implications from the Nd, Pb and Sr isotope systematics of Oldoinyo Lengai. *Journal of Petrology* **37**, 1321–1339.
- Brey, G. & Green, D. H. (1975). The role of CO<sub>2</sub> in the genesis of olivine melilitite. *Contributions to Mineralogy and Petrology* **49**, 93–103.
- Brey, G. & Green, D. H. (1977). Systematic study of liquidus phase relations in olivine melilitite + H<sub>2</sub>O + CO<sub>2</sub> at high pressures and petrogenesis of an olivine melilitite magma. *Contributions to Mineralogy and Petrology* **61**, 141–162.
- Campbell, I. A. & Griffiths, R. W. (1990). Implications of mantle plume structure for the evolution of flood basalts. *Earth and Planetary Science Letters* **99**, 79–93.
- Chandrasekaran, V., Srivastava, R. K. & Chawade, M. P. (1990). Geochemistry of the alkaline rocks of Sarnu-Dandali area, district

- Barmer, Rajasthan, India. *Journal of the Geological Society of India* **36**, 365–382.
- Church, A. A. & Jones, A. P. (1995). Silicate–carbonatite immiscibility at Oldoinyo Lengai. *Journal of Petrology* **36**, 869–889.
- Cohen, R. S. & O’Nions, K. (1982). The lead, neodymium and strontium isotopic structure of ocean ridge basalts. *Journal of Petrology* **23**, 299–324.
- Cohen, R. S., Evensen, N. M., Hamilton, P. J. & O’Nions, K. (1980). U–Pb, Sm–Nd and Rb–Sr systematics of mid-ocean ridge basalt glasses. *Nature* **283**, 149–153.
- Condomines, M., Hémond, C. & Allègre, C. J. (1988). U–Th–Ra radioactive disequilibria and magmatic processes. *Earth and Planetary Science Letters* **90**, 243–262.
- Courtilot, V., Besse, J., Vandamme, D., Jaeger, J.-J. & Montigny, R. (1986a). Les épanchements volcaniques du Deccan (Inde), cause des extinctions biologiques à la limite Crétacé–Tertiaire? *Comptes Rendus des Séances de l’Académie des Sciences, Série II* **303**(9), 863–868.
- Courtilot, V., Besse, J., Vandamme, D., Montigny, R., Jaeger, J.-J. & Cappetta, H. (1986b). Deccan flood basalt at the Cretaceous/Tertiary boundary? *Earth and Planetary Science Letters* **80**, 361–374.
- Courtilot, V., Feraud, G., Maluski, H., Vandamme, D., Moreau, M. G. & Besse, J. (1988). Deccan flood basalts and the Cretaceous/Tertiary boundary. *Nature* **333**, 843–846.
- Craig, H. & Rison, W. (1982). Helium 3; Indian Ocean hotspots and the East African Rift. *EOS Transactions, American Geophysical Union* **63**, 1144.
- Dalton, J. A. & Wood, B. J. (1993). The compositions of primary carbonate melts and their evolution through wallrock reaction in the mantle. *Earth and Planetary Science Letters* **119**, 511–525.
- Deans, T., Sukheswala, R. N., Sethna, S. F. & Viladkar, S. G. (1972). Metasomatic feldspar rocks (potash fenites) associated with the fluorite deposits and carbonatites of Amba Dongar, Gujarat, India. *Institution of Mining and Metallurgy, Transactions* **82**, B33–B40.
- Devey, C. W. & Stephens, W. E. (1992). Deccan-related magmatism west of the Seychelles–India Rift. In: Storey, B. C., Alabaster, T. & Pankhurst, R. J. (eds) *Magmatism and the Causes of Continental Break-up*. Geological Society, London, *Special Publication* **68**, 271–291.
- Dosso, L., Bougault, H., Beuzart, P., Calvez, J. Y. & Joron, J. L. (1988). The geochemical structure of the south-east Indian Ridge. *Earth and Planetary Science Letters* **88**, 47–59.
- Duncan, R. A. & Pyle, D. G. (1988). Rapid eruption of the Deccan flood basalts at the Cretaceous/Tertiary boundary. *Nature* **333**, 841–843.
- Dupré, B. & Allègre, C. J. (1983). Pb–Sr isotope variation in Indian Ocean basalts and mixing phenomena. *Nature* **303**, 142–146.
- Edgar, A. D. (1987). The genesis of alkaline magmas with emphasis on their source regions: inferences from experimental studies. In: Fitton, J. G. & Upton, B. G. J. (eds) *Alkaline Igneous Rocks*. Geological Society, London, *Special Publication* **30**, 29–52.
- Edwards, R. L., Chen, J. H. & Wasserburg, G. J. (1986).  $^{238}\text{U}$ – $^{234}\text{U}$ – $^{230}\text{Th}$ – $^{232}\text{Th}$  systematics and the precise measurement of time over the past 500,000 years. *Earth and Planetary Science Letters* **81**, 175–192.
- Eggler, D. H. (1974). Effects of  $\text{CO}_2$  on the melting of peridotite. *Carnegie Institution of Washington, Yearbook* **73**, 215–224.
- Eggler, D. H. (1978). The effect of  $\text{CO}_2$  upon partial melting of peridotite in the system  $\text{Na}_2\text{O}$ – $\text{CaO}$ – $\text{Al}_2\text{O}_3$ – $\text{MgO}$ – $\text{SiO}_2$ – $\text{CO}_2$  to 35 kb, with an analysis of melting in a peridotite– $\text{H}_2\text{O}$ – $\text{CO}_2$  system. *American Journal of Science* **278**, 305–343.
- Eggler, D. H. (1989). Carbonatites, primary melts, and mantle dynamics. In: Bell, K. (ed.) *Carbonatites: Genesis and Evolution*. London: Unwin Hyman, pp. 561–579.
- Farnetani, D. G. & Richards, M. A. (1995). Thermal entrainment and melting in mantle plumes. *Earth and Planetary Science Letters* **136**, 251–267.
- Fisk, M. R., Upton, B. G. J. & Ford, C. E. (1988). Geochemical and experimental study of the genesis of magmas of Reunion Island, Indian Ocean. *Journal of Geophysical Research* **93**, 4933–4950.
- Gerlach, D. C., Cliff, R. A., Davies, G. R., Norry, M. & Hodgson, N. (1988). Magma sources of the Cape Verdes archipelago: isotopic and trace element constraints. *Geochimica et Cosmochimica Acta* **52**, 2979–2992.
- Graham, D., Lupton, J., Albarède, F. & Condomines, M. (1990). Extreme temporal homogeneity of helium isotopes at Piton de la Fournaise, Réunion Island. *Nature* **347**, 545–548.
- Griffiths, R. W. & Campbell, I. A. (1990). Stirring and structure in mantle starting plumes. *Earth and Planetary Science Letters* **99**, 66–78.
- Grünenfelder, M. H., Tilton, G. R., Bell, K. & Blenkinsop, J. (1986). Lead and strontium isotope relationships in the Oka carbonatite complex, Quebec. *Geochimica et Cosmochimica Acta* **50**, 461–468.
- Gwalani, L. G., Rock, N. M. S., Chang, W.-J., Fernandez, S., Allègre, C. J. & Prinzhofer, A. (1993). Alkaline rocks and carbonatites of Amba Dongar and adjacent areas, Deccan Igneous Province, Gujarat, India: 1. Geology, petrography and petrochemistry. *Mineralogy and Petrology* **47**, 219–253.
- Hamelin, B. & Allègre, C. J. (1985). Large-scale regional units in the depleted upper mantle revealed by an isotope study of the South-West Indian Ridge. *Nature* **315**, 196–199.
- Hamelin, B., Dupré, B. & Allègre, C. J. (1986). Pb–Sr–Nd isotopic data of Indian Ocean ridges; new evidence of large-scale mapping of mantle heterogeneities. *Earth and Planetary Science Letters* **76**, 288–298.
- Hart, S. R. (1988). Heterogeneous mantle domains: signatures, genesis and mixing chronologies. *Earth and Planetary Science Letters* **90**, 273–296.
- Herzberg, C. (1995). Generation of plume magmas through time: an experimental perspective. *Chemical Geology* **126**, 1–16.
- Hoernle, K. A. & Tilton, G. R. (1991). Sr–Nd–Pb isotope data for Fuerteventura (Canary Islands) basal complex and subaerial volcanics: applications to magma genesis and evolution. *Schweizerische Mineralogische und Petrographische Mitteilungen* **71**, 3–18.
- Huang, Y.-M., Hawkesworth, C. J., van Calsteren, P. & McDermott, F. (1995). Geochemical characteristics and origin of the Jacupiranga carbonatites, Brazil. *Chemical Geology (Isotope Geoscience Section)* **119**, 79–99.
- Ito, E., White, W. M. & Goepel, C. (1987). The O, Sr, Nd and Pb isotope geochemistry of MORB. *Chemical Geology* **62**, 157–176.
- Jones, J. H., Walker, D., Pickett, D. A., Murrell, M. T. & Beattie, P. (1995). Experimental investigations of the partitioning of Nb, Mo, Ba, Ce, Pb, Ra, Th, Pa, and U between immiscible carbonate and silicate liquids. *Geochimica et Cosmochimica Acta* **59**, 1307–1320.
- Kalt, A., Hegner, E. & Satir, M. (1997). Nd, Sr, and Pb isotopic evidence for diverse mantle sources of East African Rift carbonatites. *Tectonophysics* **278**, 31–45.
- Kjarsgaard, B. A. & Hamilton, D. L. (1989). The genesis of carbonatites by immiscibility. In: Bell, K. (ed.) *Carbonatites: Genesis and Evolution*. London: Unwin Hyman, pp. 388–404.
- Kjarsgaard, B. A., Hamilton, D. L. & Peterson, T. D. (1995). Peralkaline nephelinite/carbonatite liquid immiscibility: comparison of phase composition in experiments and natural lavas from Oldoinyo Lengai. In: Bell, K. & Keller, J. (eds) *Carbonatite Volcanism: Oldoinyo Lengai and the Petrogenesis of Natrocarbonatites*. IAVCEI Proceedings in Volcanology **4**, 163–190.
- Klein, E. M., Langmuir, C. H., Zindler, A., Staudigel, H. & Hamelin, B. (1988). Isotope evidence of a mantle convection boundary at the Australian–Antarctic Discordance. *Nature* **333**, 623–629.

- Kramm, U. & Kogarko, L. N. (1994). Nd and Sr isotope signatures of the Khibina and Lovozero apaitic centres, Kola alkaline province, Russia. *Lithos* **32**, 225–242.
- Krishnamurthy, P., Pande, K., Gopalan, K. & Macdougall, J. D. (1988). Upper mantle xenoliths in alkali basalts related to Deccan Trap volcanism. *Geological Society of India, Memoir* **10**, 53–67.
- Kwon, S. T., Tilton, G. R. & Grünenfelder, M. H. (1989). Lead isotope relationships in carbonatites and alkalic complexes: an overview. In: Bell, K. (ed.) *Carbonatites: Genesis and Evolution*. London: Unwin Hyman, pp. 360–387.
- Le Bas, M. J. & Srivastava, R. (1989). The mineralogy and geochemistry of the Mundwara carbonatite dykes, Sirohi district, Rajasthan, India. *Neues Jahrbuch für Mineralogie, Abhandlungen* **160**, 207–227.
- le Roex, A. P. & Lanyon, R. (1998). Isotope and trace element geochemistry of Cretaceous Damaraland lamprophyres and carbonatites, northwestern Namibia: evidence for plume–lithosphere interactions. *Journal of Petrology* **39**, 1117–1146.
- Maaloe, S., James, D., Smedley, P., Petersen, S. & Garmann, L. B. (1992). The Koloa volcanic suite of Kauai, Hawaii. *Journal of Petrology* **33**, 761–784.
- Mahoney, J. J., Natland, J. H., White, W. M., Poreda, R., Bloomer, S. H., Fisher, R. L. & Baxter, A. N. (1989). Isotopic and geochemical provinces of the western Indian Ocean spreading centers. *Journal of Geophysical Research* **94**, 4033–4052.
- Manhès, G., Allègre, C. J., Dupré, B. & Hamelin, B. (1980). Lead isotope study of basic–ultrabasic layered complexes: speculations about the age of the earth and primitive mantle characteristics. *Earth and Planetary Science Letters* **47**, 370–382.
- Michard, A., Montigny, R. & Schlich, R. (1986). Geochemistry of the mantle beneath the Rodriguez triple junction and the South-East Indian Ridge. *Earth and Planetary Science Letters* **78**, 104–114.
- Milner, S. C. & le Roex, A. P. (1996). Isotope characteristics of the Okenyenya igneous complex, northwestern Namibia: constraints on the composition of the early Tristan plume and the origin of the EM I mantle component. *Earth and Planetary Science Letters* **141**, 277–291.
- Nelson, D. R., Chivas, A. R., Chappell, B. W. & McCulloch, M. T. (1988). Geochemical and isotopic systematics in carbonatites and implications for the evolution of ocean-island sources. *Geochimica et Cosmochimica Acta* **52**, 1–17.
- Newsom, H. E., White, W. M., Jochum, K. P. & Hofmann, A. W. (1986). Siderophile and chalcophile element abundances in oceanic basalts, Pb isotope evolution and growth of the Earth's core. *Earth and Planetary Science Letters* **80**, 299–313.
- Oversby, V. M. (1972). Genetic relations among the volcanic rocks of Reunion: chemical and Pb isotopic evidence. *Geochimica et Cosmochimica Acta* **36**, 1167–1179.
- Pande, K., Venkatesan, T. R., Gopalan, K., Krishnamurthy, P. & MacDougall, J. D. (1988).  $^{40}\text{Ar}$ – $^{39}\text{Ar}$  ages of alkali basalts from Kutch, Deccan volcanic province, India. *Workshop on Deccan Flood Basalts—Geological Society of India*, pp. 145–150.
- Peng, Z.-X. & Mahoney, J.-J. (1995). Drillhole lavas from the northwestern Deccan Traps, and the evolution of Réunion hotspot mantle. *Earth and Planetary Science Letters* **134**, 169–185.
- Price, R. C., Kennedy, A. K., Riggs-Sneeringer, M. & Frey, F. A. (1986). Geochemistry of basalts from the Indian Ocean triple junction; implications for the generation and evolution of Indian Ocean ridge basalts. *Earth and Planetary Science Letters* **78**, 379–396.
- Rogers, N. W., Hawkesworth, C. J. & Palacz, Z. A. (1992). Phlogopite in the generation of olivine melilitites from Namaqualand, South Africa and implications for element fractionation processes in the upper mantle. *Lithos* **28**, 347–365.
- Simonetti, A. & Bell, K. (1994a). Nd, Pb and Sr isotopic data from the Napak carbonatite–nephelinite centre, eastern Uganda: an example of open-system crystal fractionation. *Contributions to Mineralogy and Petrology* **115**, 356–366.
- Simonetti, A. & Bell, K. (1994b). Isotopic and geochemical investigation of the Chilwa Island carbonatite complex, Malawi: evidence for a depleted mantle source region, liquid immiscibility, and open-system behaviour. *Journal of Petrology* **35**, 1597–1621.
- Simonetti, A. & Bell, K. (1995). Nd, Pb and Sr isotopic data from the Mount Elgon volcano, eastern Uganda–western Kenya: implications for the origin and evolution of nephelinite lavas. *Lithos* **36**, 141–153.
- Simonetti, A., Bell, K. & Viladkar, S. G. (1995). Isotopic data from the Amba Dongar carbonatite complex, west–central India: evidence for an enriched mantle source. *Chemical Geology (Isotope Geoscience Section)* **122**, 185–198.
- Simonetti, A., Bell, K. & Shradly, C. (1997). Trace and rare-earth element geochemistry of the June 1993 natrocarbonatite lavas, Oldoinyo Lengai (Tanzania): implications for the origin of carbonatite magmas. *Journal of Volcanology and Geothermal Research* **75**, 89–106.
- Subramanyam, N. P. & Leelanandam, C. (1991). Geochemistry and petrology of the cumulo-phyric layered suite of rocks from the Toa pluton of the Mundwara alkali igneous complex, Rajasthan. *Journal of the Geological Society of India* **38**, 397–411.
- Sun, S. S. (1980). Lead isotopic study of young volcanic rocks from mid-ocean ridges, ocean islands and island arcs. In: Bailey, D. K., Tarney, J. & Dunham, K. (eds) *The Evidence for Chemical Heterogeneity in the Earth's Mantle. Philosophical Transactions of the Royal Society of London* **297**, 409–445.
- Sun, S. S. & McDonough, W. F. (1989). Chemical and isotopic systematics of oceanic basalts: implications for mantle composition and processes. In: Saunders, A. D. & Norry, M. J. (eds) *Magnetism in the Oceanic Basins. Geological Society, London, Special Publication* **42**, 313–345.
- Tilton, G. R. & Bell, K. (1994). Sr–Nd–Pb isotope relationships in Late Archean carbonatites and alkaline complexes: applications to the geochemical evolution of the Archean mantle. *Geochimica et Cosmochimica Acta* **58**, 3145–3154.
- Toyoda, K., Horiuchi, H. & Tokonami, M. (1994). Dupal anomaly of Brazilian carbonatites: geochemical correlations with hotspots in the South Atlantic and implications for the mantle source. *Earth and Planetary Science Letters* **126**, 315–331.
- Vandamme, D., Courtillot, V. & Besse, J. (1991). Paleomagnetism and age determinations of the Deccan Traps (India): results of a Nagpur–Bombay traverse and review of earlier work. *Reviews of Geophysics* **29**, 159–190.
- Veizer, J., Bell, K. & Jansen, L. A. (1993). Temporal distribution of carbonatites. *Geology* **20**, 1147–1149.
- Venkatesan, T. R., Pande, K. & Gopalan, K. (1993). Did Deccan volcanism predate the K/T transition? *Earth and Planetary Science Letters* **119**, 181–189.
- Viladkar, S. G. (1981). The carbonatites of Amba Dongar, Gujarat, India. *Bulletin of the Geological Society of Finland* **53**, 17–28.
- Wall, F., Le Bas, M. J. & Srivastava, R. K. (1993). Calcite and carbocearnite exsolution and cotectic textures in a Sr, REE-rich carbonatite dyke from Rajasthan, India. *Mineralogical Magazine* **57**, 495–513.
- Wallace, M. E. & Green, D. H. (1988). An experimental determination of primary carbonatite magma composition. *Nature* **335**, 343–346.
- White, W. M. & Patchett, J. (1984). Hf–Nd–Sr isotopes and incompatible element abundances in island arcs: implications for magma origins and crust–mantle evolution. *Earth and Planetary Science Letters* **67**, 167–185.

Wilson, M., Rosenbaum, J. M. & Dunworth, E. A. (1995). Melilitites: partial melts of the thermal boundary layer? *Contributions to Mineralogy and Petrology* **119**, 181–196.

Woolley, A. R. & Kempe, D. R. C. (1989). Carbonatites: nomenclature, average chemical compositions, and element distribution. In: Bell, K. (ed.) *Carbonatites: Genesis and Evolution*. London: Unwin Hyman, pp. 1–14.